Fermi National Accelerator Laboratory

FN-472
[SSC-161]

Linear Beam-Beam Effects for Round Beams

King-Yuen Ng
SSC-CDG, Lawrence Berkeley Laboratory
90/4040, Berkeley, California 94720
and
Fermi National Accelerator Laboratory
P.O. Box 500, Batavia, Illinois 60510

January 1988

Operated by Universities Research Association Inc. under contract with the United States Department of Energy

SSC-161

FN-472

January, 1988

LINEAR BEAM-BEAM EFFECTS FOR ROUND BEAMS

King-Yuen Ng

SSC-CDG, Lawrence Berkeley Laboratory 90/4040, Berkeley, CA 94720

and

Fermi National Accelerator Laboratory, Batavia, IL 60510

I. INTRODUCTION

The luminosity of a collider is limited by the beam-beam interactions. When the beam current is small, the beam-beam tune shift or perturbed beam-beam parameter increases steadily with the current and as does the luminosity. However, when the beam current is big enough, several things will happen. One bunch may increase in size while the other will not. This situation, known as flip-flop, requires a bifurcation solution for explanation. This will lower the perturbed beam-beam parameter and therefore the luminosity. Direct flip-flop had been observed in SPEAR by Paterson and Donald.[1] A drop in the beam-beam tune shift had been recorded in PETRA by Piwinski (Fig. 1).[2] Of course, the drop in beam-beam tune shift need not be a result of the flip-flop phenomenon. Both bunches may also blow up in size but will remain stable. The luminosity will undoubtedly be lowered. Finally, one or both bunches may blow up indefinitely and will be lost eventually.

We study beam-beam collision for two gaussian bunches having circular transverse cross sections. We follow the mapping method proposed by Hirata,[3] who studied a flat beam with a nonlinear beam-beam kick. However, here the beam-beam kick is assumed to be linear.[4] Of course, this assumption is not physical especially for particles near the edge of a bunch. However, this model has three points of merit. First, the particle distribution remains gaussian after each collision. Second, this model is symplectic when radiation damping is neglected.[4] Third, this model can be solved analytically up to a certain extent. For this reason, we deem this model worthy of investigation.

In our results, there is stable period-one fixed-point bifurcation only when the residual tune ν is between 0.25 and 0.5 or between 0.75 and 1. However, for tune values between 0 and 0.25 or between 0.5 and 0.75, there is no bifurcation, but the period-one fixed point splits up into period-three fixed point as the beam-beam parameter increases. However, this can also serve as an explanation of Piwinski's observation[2] of a sudden decrease in luminosity. In contrast, Hirata's results[3] exhibit bifurcation for all tune values.

The model is reviewed in Section II and the period-one fixed point solution is solved analytically in Section III. In Section IV, the stability of the solution is studied analytically using the stability matrix. In Section V, numerical tracking is used to study higher-period fixed points.

II. THE MODEL

We follow closely the model in Ref. 3 and the notations therein. Consider the motion of a particle in a bunch in the vertical direction y. Since the transverse cross

section of the bunch is assumed circular, motion in the horizontal direction x can be treated identically if beta-sychrotron coupling is neglected.

Denote the canonical variables in terms of nominal Twiss parameters by $Y_1 = y/\sqrt{\beta_y}$ and $Y_2 = (\alpha_y + \beta_y y')\sqrt{\beta_y}$. Here, β_y and α_y are Twiss parameters and y' denotes the angle the particle's path makes with the ideal orbit. We are interested only in the statistical quantities such as the averages of the moments $Y_i Y_j$ denoted by $\Lambda_{ij} = \langle Y_i Y_j \rangle$. For the partner bunch, these quantities carry an asterisk as a superscript.

The motion of the particle can be described by successive operations:

B (beam-beam force)

$$\begin{pmatrix} Y_1' \\ Y_2' \end{pmatrix} = \begin{pmatrix} 1 & 0 \\ -\kappa/\Lambda_{11}^* & 1 \end{pmatrix} \begin{pmatrix} Y_1 \\ Y_2 \end{pmatrix} ,$$

R (radiation)

$$\begin{pmatrix} Y_1' \\ Y_2' \end{pmatrix} = \begin{pmatrix} 1 & 0 \\ 0 & \lambda \end{pmatrix} \begin{pmatrix} Y_1 \\ Y_2 \end{pmatrix} + \sqrt{(1-\lambda^2)\epsilon}\hat{r} \begin{pmatrix} 1 \\ 1 \end{pmatrix} ,$$

O (betatron oscillation)

$$\begin{pmatrix} Y_1' \\ Y_2' \end{pmatrix} = U \begin{pmatrix} Y_1 \\ Y_2 \end{pmatrix} = \begin{pmatrix} \cos\mu & \sin\mu \\ -\sin\mu & \cos\mu \end{pmatrix} \begin{pmatrix} Y_1' \\ Y_2' \end{pmatrix} , \tag{2.1}$$

where $\mu = 2\pi\nu$ is the phase advanced from one interaction point to the next, $\lambda = \exp(-2/T_0)$ is the damping ratio with T_0 the damping time in units of propagation time between two interaction points, $\epsilon = \epsilon_y$ is the nominal vertical emittance, $\hat{r}$ is a gaussian noise with unit standard deviation, $\kappa = 4\pi\eta$, and the nominal beam-beam parameter is defined as

$$\eta = \frac{N r_p}{2\pi\gamma\epsilon_y} . \tag{2.2}$$

In the above, N is the number of particles in each bunch, r_p is the classical electromagnetic particle radius, γ is the relativistic Lorentz factor, and Note that for a round beam $\epsilon_x\beta_x = \epsilon_y\beta_y$, where $\beta_{x,y}$ is the nominal beta function at the interaction point. Here, the effects of radiation and diffusion have been treated locally as a lumped sum at the interaction point.

In this model, the statistical moments Λ_{ij} transform according to Eq. (2.1) as

$$
\begin{aligned}
B: \quad & \Lambda'_{11} = \Lambda_{11} \ , \quad \Lambda'_{12} = \Lambda_{12} - \frac{\kappa\Lambda_{11}}{\Lambda^*_{11}} \ , \quad \Lambda'_{22} = \Lambda_{22} - \frac{2\kappa\Lambda_{12}}{\Lambda^*_{11}} + \frac{\kappa^2\Lambda_{11}}{\Lambda^{*2}_{11}} \ , \\
R: \quad & \Lambda'_{11} = \Lambda_{11} \ , \qquad \Lambda'_{12} = \lambda\Lambda_{12} \ , \qquad \Lambda'_{22} = \lambda^2\Lambda_{22} + (1-\lambda^2)\epsilon \ , \\
O: \quad & \Lambda' = \tilde{U}\Lambda U \ .
\end{aligned}
\tag{2.3}
$$

Note that $\det \Lambda$ is invariant for operations B and O. This is also true for the operation R if radiation damping is neglected ($\lambda = 1$); then the whole transformation $B \rightarrow R \rightarrow O$ will be symplectic. This is also evident in Eq. (2.1).

III. PERIOD-ONE FIXED POINT

The period-one fixed point is defined as the solution that is invariant after the passage from one interaction point to the next. If it is stable, this is what we observe.

The period-one fixed point (just before B) can be solved easily. Let $z = \cot\mu$,

$$
t = \frac{8\pi\eta\lambda}{1+\lambda} \ , \tag{3.1}
$$

and the ratio of bunch sizes $R = \Lambda_{11}/\Lambda^*_{11}$. The period-one fixed point is

$$
\Lambda_{11}(R) = \frac{\epsilon R}{2}\left\{\left(\frac{1}{R} - tz\right) + \left[\left(\frac{1}{R} - tz\right)^2 + t^2\right]^{1/2}\right\} \ ,
$$

$$
\Lambda_{12}(R) = \frac{tR}{2} \ ,
$$

$$
\Lambda_{22}(R) = \epsilon + \frac{\Lambda^2_{12}}{\Lambda_{11}} \ ,
$$

and

$$
\Lambda^*_{ij}(R) = \Lambda_{ij}(R^{-1}) \ . \tag{3.2}
$$

It is interesting to note that the solution depends on t only which is very nearly equal to $4\pi\eta$ and is not sensitive to λ at all, although in deriving the solution we definitely require $\lambda \neq 1$. The above solution is obtained by setting the changes of $\det\Lambda$, $\mathrm{Tr}\,\Lambda$, and Λ_{11} to zero for the series of operations $B \rightarrow R \rightarrow O$, and then determining the sign of Λ_{12} by solving another equation (since $\det\Lambda$ cannot fix the sign of Λ_{12}). The ratio between the bunch sizes can then be obtained by solving the self-consistent equation,

$$
R = \frac{\Lambda_{11}(R)}{\Lambda^*_{11}(R)} \ . \tag{3.3}
$$

Obviously, if R is a solution so is $1/R$ also. It is easy to see that $R = 0,\ 1,\ \infty$ are solutions. However, when $t_b < t < t_e$, where

$$t_b = \frac{z + \sqrt{3 + 4z^2}}{1 + z^2} \qquad \text{and} \qquad t_e = 2(z + \sqrt{1 + z^2}) \ , \tag{3.4}$$

there exists another solution

$$R = b \pm \sqrt{b^2 - 1} \ , \qquad b = \frac{t^2(1 + 2z^2) - 2}{4 + 4tz - t^2} \ . \tag{3.5}$$

Starting from $t = t_b$ where $b = 1$, R bifurcates into two branches which approach ∞ and 0 as $t \to t_e$. When $t > t_e$, there is no more bifurcation and the only solution is that of the $R = 1$. These are all the period-one fixed point solutions of the problem. They are displayed in Fig. 2. We want to point out that there is no finite t_e in Hirata's results.[3] In other words, the bifurcation continues as the beam parameter increases.

It appears that we have obtained a bifurcation solution in a simple analytic form. Unfortunately, the stability analysis and numerical tracking of Sections IV and V show that the bifurcation solution is stable only when $z < 0$ or when the residual tune satisfies $0.25 < \nu < 0.5$ or $0.75 < \nu < 1.0$. Even in these regions, the beam-beam parameter range of the bifurcation from t_b to t_e is extremely narrow. For the other regions of the residual tune, the only stable solution is $R = 1$ when t is small, and instability sets in well before the bifurcation point t_b. However, Hirata[3] obtains stable bifurcation for all values of ν.

By numerical tracking, we mean starting from a set of Λ_{ij} and Λ^*_{ij} that deviates from a solution by a small amount and apply the $B \to R \to O$ operations many times numerically. Λ_{ij} and Λ^*_{ij} should converge to the solution values after many turns if the solution is stable, otherwise it is unstable.

In passing, we want to show the positions of the solutions in the complex R-plane. At $t = 0$, we have solutions at 0, 1, ∞, and $(1 \pm \sqrt{3})/2$; the last two are of course unphysical. As t increases, the two complex solutions move along the unit circle and reach $R = 1$ when $t = t_b$. Two of these three solutions at $R = 1$ then move along the real R-axis reaching zero and infinity at $t = t_e$ giving the bifurcation solution. The third one remains at $R = 1$ (see Fig. 3).

IV. THE STABILITY MATRIX

If we consider Λ_{11}, Λ_{12}, Λ_{22}, Λ^*_{11}, Λ^*_{12}, Λ^*_{22} as a column matrix, the $B \to R \to O$ operation implies the transformation

$$\begin{pmatrix} \Lambda' \\ \Lambda^{*\prime} \end{pmatrix} = \begin{pmatrix} \mathcal{M}(\Lambda*) & 0 \\ 0 & \mathcal{M}(\Lambda) \end{pmatrix} \begin{pmatrix} \Lambda \\ \Lambda^* \end{pmatrix} + \dots \ , \tag{4.1}$$

where the remaining term denotes the diffusion of the R operation. In Eq. (4.1),

$$\Lambda = \begin{pmatrix} \Lambda_{11} \\ \Lambda_{12} \\ \Lambda_{22} \end{pmatrix} , \qquad \Lambda^* = \begin{pmatrix} \Lambda^*_{11} \\ \Lambda^*_{12} \\ \Lambda^*_{22} \end{pmatrix} , \tag{4.2}$$

and the 3×3 matrix $\mathcal{M}(\Lambda^*)$ can be written explicitly as

$$\mathcal{M}(\Lambda^*) = \begin{pmatrix} c^2 - \dfrac{2\lambda\kappa sc}{\Lambda^*_{11}} + \dfrac{\lambda^2\kappa^2 s^2}{\Lambda^{*2}_{11}} & 2\lambda sc - \dfrac{2\lambda^2\kappa s^2}{\Lambda^*_{11}} & \lambda^2 s^2 \\ -\dfrac{\lambda\kappa(c^2-s^2)}{\Lambda^*_{11}} - sc\left(1 - \dfrac{\lambda^2\kappa^2}{\Lambda^{*2}_{11}}\right) & \lambda(c^2-s^2) - \dfrac{2\lambda^2\kappa sc}{\Lambda^*_{11}} & \lambda^2 sc \\ s^2 + \dfrac{2\lambda\kappa sc}{\Lambda^*_{11}} + \dfrac{\lambda^2\kappa^2 c^2}{\Lambda^{*2}_{11}} & -2\lambda sc - \dfrac{2\lambda^2\kappa c^2}{\Lambda^*_{11}} & \lambda^2 c^2 \end{pmatrix} , \tag{4.3}$$

with $s = \sin\mu$ and $c = \cos\mu$. If Λ_{ij} and Λ^*_{ij} deviate from a period-one fixed point by an infinitesimal amount $\Delta\Lambda_{ij}$ and $\Delta\Lambda^*_{ij}$, the corresponding changes in Λ'_{ij} and $\Lambda^{*\prime}_{ij}$ are given by

$$\begin{pmatrix} \Delta\Lambda'_{ij} \\ \Delta\Lambda^{*\prime}_{ij} \end{pmatrix} = \begin{pmatrix} \mathcal{M}(\Lambda^*) & \bar{\mathcal{M}}(\Lambda,\Lambda^*) \\ \bar{\mathcal{M}}(\Lambda^*,\Lambda) & \mathcal{M}(\Lambda) \end{pmatrix} \begin{pmatrix} \Delta\Lambda_{ij} \\ \Delta\Lambda^*_{ij} \end{pmatrix} , \tag{4.4}$$

where

$$\bar{\mathcal{M}}(\Lambda,\Lambda^*)_{ij} = \sum_k \frac{\partial\mathcal{M}(\Lambda^*)_{ik}}{\partial\Lambda^*_{11}}\Lambda_{kj}\delta_{j1} , \tag{4.5}$$

with the indices running over 1, 2, 3 denoting (11), (12), (22) respectively. Explicitly,

$$\bar{\mathcal{M}}(\Lambda,\Lambda^*) = \begin{pmatrix} \dfrac{2\lambda\kappa sc\Lambda_{11}}{\Lambda^{*2}_{11}} - \dfrac{2\lambda^2\kappa^2 s^2\Lambda^2_{11}}{(1+\lambda)\Lambda^{*3}_{11}} & 0 & 0 \\ \dfrac{\lambda\kappa(c^2-s^2)\Lambda_{11}}{\Lambda^{*2}_{11}} - \dfrac{2\lambda^2\kappa^2 sc\Lambda^2_{11}}{(1+\lambda)\Lambda^{*3}_{11}} & 0 & 0 \\ -\dfrac{2\lambda\kappa sc\Lambda_{11}}{\Lambda^{*2}_{11}} - \dfrac{2\lambda^2\kappa^2 c^2\Lambda^2_{11}}{(1+\lambda)\Lambda^{*3}_{11}} & 0 & 0 \end{pmatrix} . \tag{4.6}$$

Both the four 3×3 matrices in Eq. (4.4) are evaluated at the fixed-point values. To test the stability of the fixed point, what we need is to compute the six eigenvalues of the 6×6 matrix and see whether they have magnitudes less than unity. We show in the Appendix that the eigenvalue x can be obtained by solving the following indicial

equation,

$$\det M(\Lambda^*)\det M(\Lambda) - \det N(\Lambda,\Lambda^*)\det N(\Lambda^*,\Lambda) = 0 \ , \tag{4.7}$$

where the 3×3 matrices $M(\Lambda^*)$ and $M(\Lambda)$ are the same as $\mathcal{M}(\Lambda^*)$ and $\mathcal{M}(\Lambda)$ in Eq. (4.2) except that $-x$ is added onto each diagonal element. The 3×3 matrices $N(\Lambda,\Lambda^*)$ and $N(\Lambda^*,\Lambda)$ are the same as $M(\Lambda^*)$ and $M(\Lambda)$ except that their first columns are replaced by the first columns of $\bar{\mathcal{M}}(\Lambda,\Lambda^*)$ and $\bar{\mathcal{M}}(\Lambda^*,\Lambda)$ respectively.

Let us first study the situation of $R = 1$, since this can give us information of the stability of the bifurcation solution. With $R = 1$, we have

$$M = M(\Lambda^*) = M(\Lambda) \ ,$$

$$N = N(\Lambda,\Lambda^*) = N(\Lambda^*,\Lambda) \ , \tag{4.8}$$

and Eq. (4.7) splits up into

$$\det M + \det N = 0 \ , \tag{4.9}$$

$$\det M - \det N = 0 \ , \tag{4.10}$$

where actually Eq. (4.9) corresponds to the situation $\Delta\Lambda_{ij} = \Delta\Lambda^*_{ij}$ and Eq. (4.10) corresponds to the situation $\Delta\Lambda_{ij} = -\Delta\Lambda^*_{ij}$. These are cubic equations and can therefore be solved in the closed form. However, since the matrix elements are not sensitive to damping, it is a good idea to set $\lambda \to 1$ and obtain a much simplified solution. Now the system is stable when each of the three roots of Eqs. (4.9) and (4.10) lie on a unit circle. Therefore, for each equation, we expect one root to be unity and stay fixed while the other two are complex when we have stability but becoming real when stability is lost. In fact, this turns out to be the actual situation. Thus each cubic reduces to a quadratic equation only.

We want to list M and N in the simplified form

$$M = \begin{pmatrix} (c-\alpha s)^2 - x & 2s(c-\alpha s) & s^2 \\ -(c-\alpha s)(s+\alpha c) & -2s(s+\alpha c) + 1 - x & sc \\ (s+\alpha c)^2 & -2c(s+\alpha c) & c^2 - x \end{pmatrix} \ ,$$

$$N = \begin{pmatrix} \alpha s(2c-\alpha s) & 2s(c-\alpha s) & s^2 \\ \alpha(c^2-s^2) - \alpha^2 sc & -2s(s+\alpha c) + 1 - x & sc \\ -\alpha c(2s+\alpha c) & -2c(s+\alpha c) & c^2 - x \end{pmatrix} \ , \tag{4.11}$$

where $\alpha = t/\Lambda_{11}$ since $t = \kappa$ in the limit $\lambda \to 1$.

For $\Delta\Lambda_{ij} = \Delta\Lambda^*_{ij}$, Eq. 4.9 gives

$$x = 1,\ 1 - a \pm i\sqrt{a(2-a)} \tag{4.12}$$

with $a = s(2s + \alpha c)$. The parameter t is related to α by

$$t = \frac{4\alpha}{4 + 4\alpha z - \alpha^2}\ , \tag{4.13}$$

which is a monotonic increasing function of α, except at two points $\alpha = 2z \pm 2\sqrt{z^2+1}$ where t diverges. Therefore, the value of α cannot exceed $2z + 2\sqrt{z^2+1}$ physically. The condition for stability is

$$\begin{cases} 0 \le \alpha \le 2z & z > 0 \\ 0 \le \alpha \le 2z + 2\sqrt{z^2+1} & z < 0\ . \end{cases} \tag{4.14}$$

Together with Eq. (4.13), these limits can be rewritten as

$$\begin{cases} 0 \le t \le \dfrac{2z}{1+z^2} & z > 0 \ \text{ or } \ 0 < \nu < \frac{1}{4} \\ 0 \le t \le \infty & z < 0 \ \text{ or } \ \frac{1}{4} < \nu < \frac{1}{2}\ , \end{cases} \tag{4.15}$$

where ν is the residual tune.

For $\Delta\Lambda_{ij} = -\Delta\Lambda^*_{ij}$, Eq. (4.10) gives

$$x = 1,\ 1 - a' \pm i\sqrt{a'(2-a')}\ , \tag{4.16}$$

where $a' = 2s^2 + 3\alpha sc - \alpha^2 s^2$. Stability requires

$$\begin{cases} 0 \le \alpha \le z & z > 0 \\ 0 \le \alpha \le \dfrac{3z}{2} + \dfrac{1}{2}\sqrt{9z^2+8} & z < 0\ . \end{cases} \tag{4.17}$$

They imply

$$\begin{cases} 0 \le t \le \dfrac{4z}{4+3z^2} & z > 0 \ \text{ or } \ 0 < \nu < \frac{1}{4} \\ 0 \le t \le \dfrac{z + \sqrt{9z^2+8}}{1+z^2} & z < 0 \ \text{ or } \ \frac{1}{4} < \nu < \frac{1}{2}\ . \end{cases} \tag{4.18}$$

Comparing Eqs. (4.14) and (4.17) or (4.15) and (4.18), it is evident that the limits for $\Delta\Lambda_{ij} = -\Delta\Lambda_{ij}^*$ are more stringent than those for $\Delta\Lambda_{ij} = \Delta\Lambda_{ij}^*$. Thus, in general the period-one fixed point will become unstable at the upper limits of Eq. (4.18).

We denote the stability limit for $R = 1$ (and also $\lambda = 1$) by t_s. Comparing t_s of Eq. (4.18) with the onset of the bifurcation solution t_b of Eq. (3.4), we get

$$t_b > t_s \qquad z > 0 \text{ or } 0 < \nu < \tfrac{1}{4}\,, \tag{4.19}$$

$$t_b < t_e < t_s \qquad z < 0 \text{ or } \tfrac{1}{4} < \nu < \tfrac{1}{2}\,, \tag{4.20}$$

Equation (4.19) says that, for $0 < \nu < 0.25$, the $R = 1$ solution becomes unstable at $t = t_s$ which is before the onset of the bifurcation solution. This implies that the bifurcation solution would be unstable. On the other hand, when $0.25 < \nu < 0.5$, the $R = 1$ solution is still stable after passing the point of bifurcation. This implies that the bifurcation solution would probably be stable also up to the end point t_e. These assertions can be verified by studying the eigenvalues of the stability matrix (4.3) for the situation when $R \neq 1$. But we have to face a sixth-order indicial equation which can be reduced at most to a quartic equation if we put $\lambda = 1$. Analytic solution is theoretically possible. However, the complexity of the resulting expressions would prevent us from drawing any conclusion.

An easier way is to resort to numerical solution. Our assertion is indeed correct when damping is neglected ($\lambda = 1$), i.e., the bifurcation solution is unstable for $0 < \nu < 0.25$ but becomes stable when $0.25 < \nu < 0.5$. This is still true when damping is introduced. However the $R = 1$ solution for $0.25 < \nu < 0.5$ becomes unstable when t reaches t_s, the onset of bifurcation. This implies that there is at most one stable solution for each t. In this range of ν, when t is small we have the $R = 1$ solution and it starts to bifurcate at $t = t_b$. When $t > t_e$ there is no more stable solution. On the other hand, for $0 < \nu < 0.25$, there is only the $R = 1$ solution which becomes unstable when $t > t_s$. The above results are summarized in Fig. 4.

V. NUMERICAL TRACKING

So far we have studied only period-one fixed points. There are also period-two, period-three, and higher-period fixed points. Under some particular situations, these higher-period fixed points may be more stable than the period-one fixed points. That explains why we meet with points of instability. Analytical study of higher-period fixed points is very difficult because the mapping, as shown in Eq. (2.3), is nonlinear. For this reason, numerical tracking in the sense stated in Section III is performed

instead. Of course, numerical tracking can also help us to verify the stability or instability of the bifurcation solution.

First, let us study the case where residual tune $\nu = 0.15$ and damping time $T_0 = 142.9$ or $\lambda = 0.9861$. We find that the period-one fixed point is stable up to $t = 0.525$ exactly as given by Eq. (4.18). After that the solution converges to period-three fixed points instead as shown in Fig. 5. If t increases continuously and becomes sufficiently large, it is possible that the stable solution goes to something like period-seven fixed points, or we even have one beam divergent while the other stable but fluctuating. For this tune value, there is no stable bifurcation solution.

We can define a perturbed beam-beam parameter

$$\xi = \frac{2\epsilon\eta}{\Lambda_{11} + \Lambda_{11}^*} , \tag{5.1}$$

so that the luminosity becomes $L = L_0\xi/\eta$ where L_0 is the unperturbed luminosity. If the harmonic mean $\Lambda_{11}^{\mathrm{harm}}$ of the three period-three fixed points $\Lambda_{11}^{(i)}$, defined as

$$\frac{1}{\Lambda_{11}^{\mathrm{harm}}} = \frac{1}{3}\sum_{i=1}^{3}\frac{1}{\Lambda_{11}^{(i)}} , \tag{5.2}$$

is taken as Λ_{11} or Λ_{11}^* in Eq. (5.1), the plot of ξ against η in Fig. 6 shows a sudden decrease of ξ or luminosity at $t = 0.5205$ or $\eta = 0.0414$. Here, the decrease is a discontinuity because the beam sizes change from the period-one fixed-point solution to the period-three fixed-point solution abruptly. The peak value of ξ is 0.059. This may serve as an explanation of Piwinski's observation and the values of η and ξ are also of the right order of magnitude.

For the period-one fixed point, since $\Lambda_{11} \propto t$ or η for large t, ξ will be saturated for large η at $\xi = [4\pi(-z+\sqrt{1+z^2})]^{-1}$. The saturation seen experimentally, however, is definitely not this saturation value because period-one fixed point becomes unstable at very early t when ξ is still very small.

It is worth pointing out that the final equilibrium solution depends on the history of the beam. If we increase t or the current slowly, the solution changes from period-one fixed point to period-three fixed points at $t = 0.5205$. However, if we let t decrease gradually now, the solution will stick to period-three fixed points even when t is less than 0.5205. The solution goes back to period-one fixed point only when t is sufficiently small. The reason for this peculiar behavior is that there is a region of stability for the period-one fixed point and also for the period-three fixed points although that region may be very small. Therefore the solution may converge to a certain fixed point if we are near enough to it unless there exists no stability region at all or that fixed point is completely unstable.

We do numerical tracking also for $\nu = 0.2$ and $T_0 = 142.9$. Here, the limits for $\Delta\Lambda_{ij} = \pm\Delta\Lambda_{ij}^*$ are $t = 0.3011$ and 0.5878 respectively. If we keep $\Delta\Lambda_{ij} = \Delta\Lambda_{ij}^*$, which is impossible to do experimentally, the period-one fixed point starts to "bifurcate" into period-two fixed points at $t = 0.5878$ and later into period-four fixed points as shown in Fig. 7. However, if we begin with $\Delta\Lambda_{ij} \neq \Delta\Lambda_{ij}^*$, which is what we have in experimental operation, the stable period-one fixed point starts chaotic behavior after $t = 0.3011$ and continues so even after $t = 0.5878$ (Fig. 8). One possible reason may be that the period-three fixed points are too far away and their stability region is too small. When we compute the average beam size, we find that Λ_{11} jumps from the period-one fixed point value of ~ 0.93 to a value ranging from ~ 1.8 to 2.8. This will certainly lower the perturbed beam-beam parameter ξ, but the effect is not big.

We next explore the situation when the residual tune is between 0.25 and 0.5 or between 0.75 and 1. We find that when $t_b < t < t_e$, the convergence to the stable bifurcation solution is extremely slow. This is expected as we recall that the $R = 1$ solution is *just stable* when $\lambda \to 1$. Beyond t_e, the $R = 1$ solution is not stable. But the divergence is extremely slow too because of the same reason. Here we do not encounter any higher-order fixed points. When t exceeds t_s, the stability point for $\Delta\Lambda_{ij} = -\Delta\Lambda_{ij}^*$, numerical tracking shows a fast divergence of one beam without encountering any higher-order fixed point also.

VI. CONCLUSION

We have studied the beam-beam interaction using a simple round beam model with linear beam-beam kick. The results are interesting and are summarized in Fig. 4:

(1) The region under the solid curve is completely stable.

(2) When the residual tune ν is between 0 and 0.25 (or 0.5 and 0.75), if the beam current is high enough so that $t > t_s$, the bunch sizes may converge to period-three fixed points. The observation will be the blow up of both bunches. This can explain the drop in perturbed beam-beam tune shift or luminosity. It may also happen that the period-three fixed points are too far away from the period-one fixed point. The bunch sizes then fluctuate and become chaotic. The result may lead to a slight drop in luminosity and eventual instability.

(3) When the residual tune ν is between 0.25 and 0.5 (or 0.75 and 1), as the beam current increases, the bunches may enter the stable bifurcation or flip-flop region if $t_b < t < t_e$. If $t > t_e$, one or both bunches will blow up and become unstable.

Part of this work was done at KEK National Laboratory for High Energy Physics in Japan and the SSC Central Design Group at Berkeley. The author would like to thank Professor Y. Kimura and the KEK Accelerator Theory Group for their invitation and their hospitality during his stay. He is grateful to Professor M. Tigner and Dr. A. Chao for their invitation and hospitality. He would also like to acknowledge the fruitful discussions made with Professor K. Hirata, Professor K. Yokoya, Dr. A. Chao, and Dr. M. Furman.

APPENDIX

We want to compute the determinant of a 6×6 matrix $\mathcal{M}$ which has the form

$$\mathcal{M} = \begin{pmatrix} & & a_1 & 0 & 0 \\ & M(\Lambda^*) & a_2 & 0 & 0 \\ & & a_3 & 0 & 0 \\ b_1 & 0 & 0 & & \\ b_2 & 0 & 0 & M(\Lambda) & \\ b_3 & 0 & 0 & & \end{pmatrix}, \tag{A.1}$$

where $M(\Lambda^*)$ and $M(\Lambda)$ are 3×3 matrices. The determinant can be written as

$$\begin{aligned} \det \mathcal{M} \;=\; & \det \begin{pmatrix} M(\Lambda^*) & 0 \\ 0 & M(\Lambda) \end{pmatrix} + \det \begin{pmatrix} & a_1 & 0 & 0 \\ M(\Lambda^*) & a_2 & 0 & 0 \\ & a_3 & 0 & 0 \\ & 0 & \times & \times \\ 0 & 0 & \times & \times \\ & 0 & \times & \times \end{pmatrix} \\ & + \det \begin{pmatrix} 0 & \times & \times & & \\ 0 & \times & \times & 0 & \\ 0 & \times & \times & & \\ b_1 & 0 & 0 & & \\ b_2 & 0 & 0 & M(\Lambda) & \\ b_3 & 0 & 0 & & \end{pmatrix} + \det \begin{pmatrix} 0 & \times & \times & a_1 & 0 & 0 \\ 0 & \times & \times & a_2 & 0 & 0 \\ 0 & \times & \times & a_3 & 0 & 0 \\ b_1 & 0 & 0 & 0 & \times & \times \\ b_2 & 0 & 0 & 0 & \times & \times \\ b_3 & 0 & 0 & 0 & \times & \times \end{pmatrix}, \end{aligned} \tag{A.2}$$

where the lower-right-hand 3×3 matrix in the second term on the right side denotes $M(\Lambda)$ with its first column replaced by zeroes, and the upper-left-hand 3×3 matrix in the third term denotes $M(\Lambda^*)$ with its first column replaced by zeroes. It can be shown easily that the second and third determinants on the right side vanish. The

last determinant can be rewritten as

$$-\det\begin{pmatrix} a_1 & \times & \times & & \\ a_2 & \times & \times & 0 & \\ a_3 & \times & \times & & \\ & & & b_1 & \times & \times \\ & 0 & & b_2 & \times & \times \\ & & & b_3 & \times & \times \end{pmatrix} = -\det\begin{pmatrix} N(\Lambda,\Lambda^*) & 0 \\ 0 & N(\Lambda^*,\Lambda) \end{pmatrix}, \quad \text{(A.3)}$$

where $N(\Lambda^*)$ and $N(\Lambda)$ are the same as $M(\Lambda^*)$ and $M(\Lambda)$ but with their first columns replaced by

$$\begin{pmatrix} a_1 \\ a_2 \\ a_3 \end{pmatrix} \quad \text{and} \quad \begin{pmatrix} b_1 \\ b_2 \\ b_3 \end{pmatrix}$$

respectively. Therefore, we get

$$\det \mathcal{M} = \det M(\Lambda^*)\det M(\Lambda) - \det N(\Lambda,\Lambda^*)\det N(\Lambda^*,\Lambda) \ .$$

REFERENCES

1. J. M. Paterson and M. Donald, in *Proc. 1979 Accelerator Conference*, San Francisco, March 12-14, 1979.

2. A. Piwinski, in *Proc. 11th Int. Conf. on High Energy Accelerators*, Geneva, July 1980, p.751 (Birkhäuser 1980).

3. K. Hirata, Phys. Rev. Lett. **58**, 25 (1987) and KEK-87-76.

4. A. Chao and M. Furman also studied such a linear model but for a flat beam, (to be published as a SSC report). They pointed out that for a linear kick, because a gaussian bunch distribution remains gaussian after each collision, the symplecticity of the problem will be maintained if radiation damping is neglected. For a flat beam, however, their results are not as simple as ours.

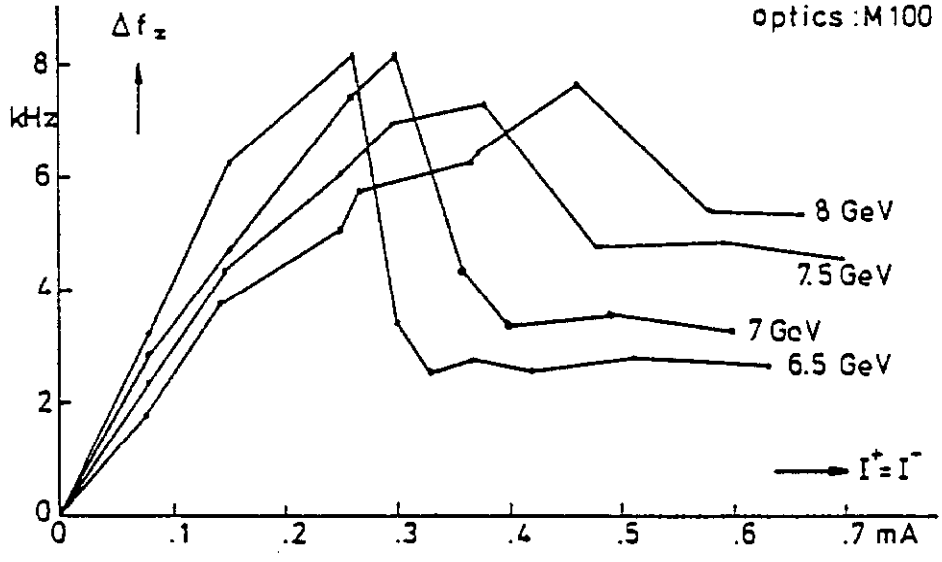

Figure 1. Vertical frequency splitting verses beam current at PETRA, showing a sudden drop in the splitting.

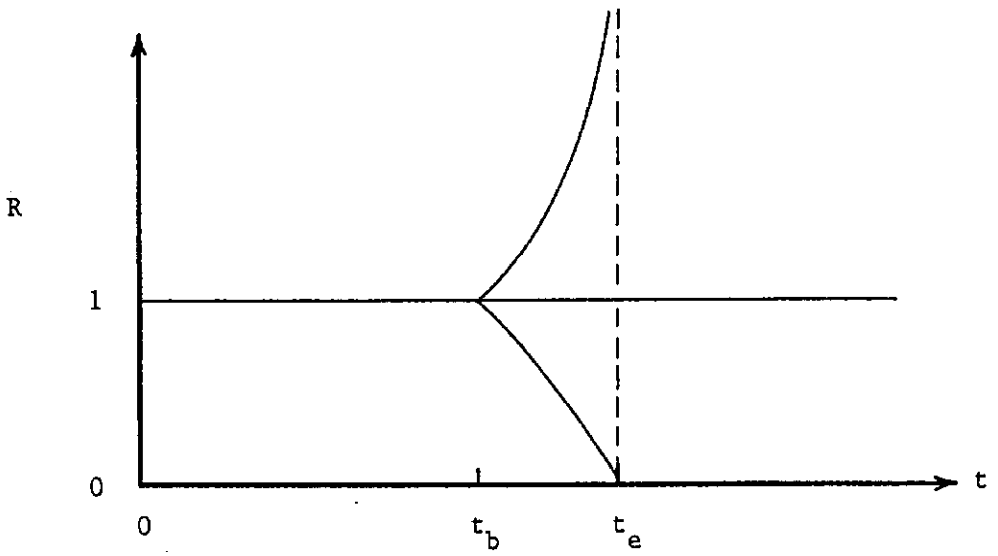

Figure 2. Period-one fixed point solutions.

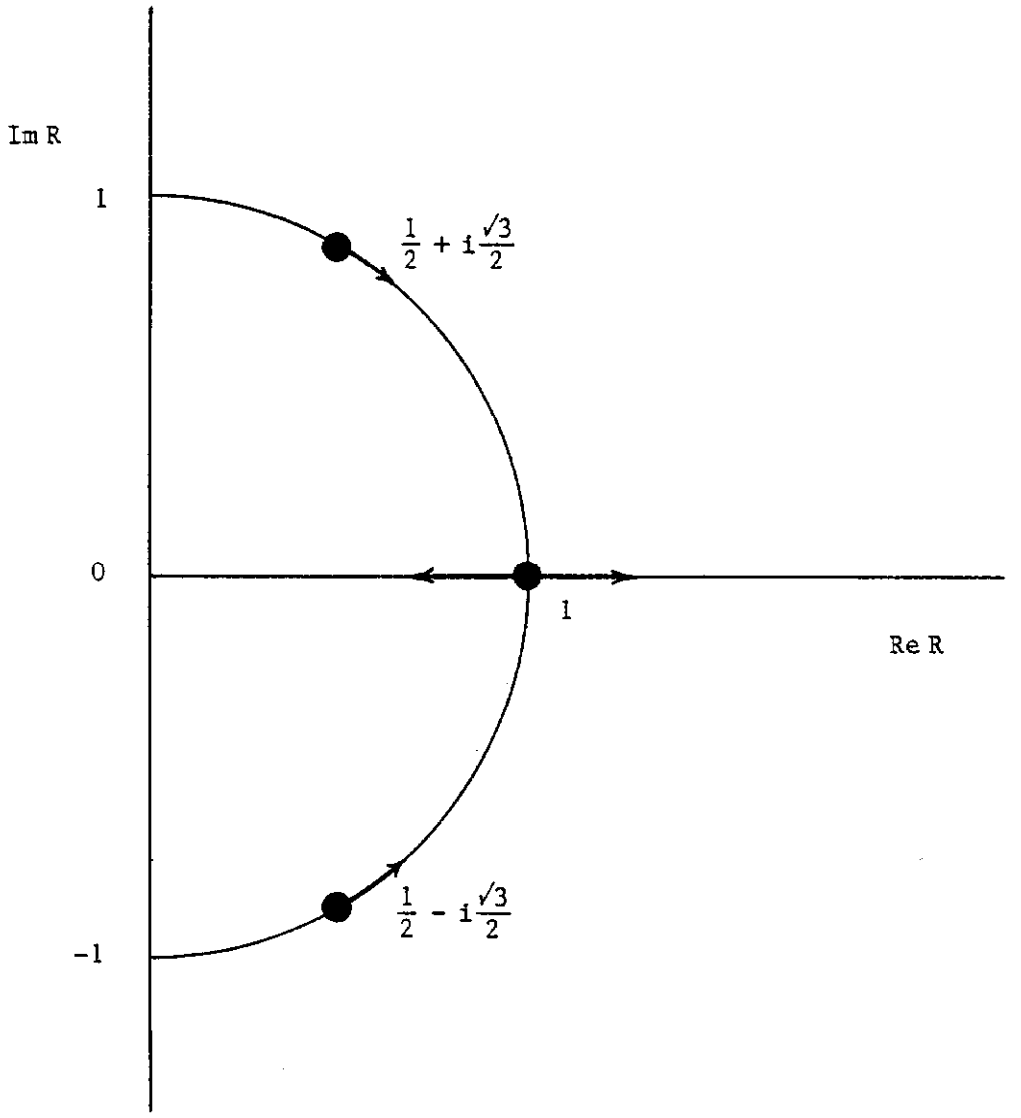

Figure 3. Movement of the period-one fixed point solutions in the complex R-plane as t increases from 0 to t_e.

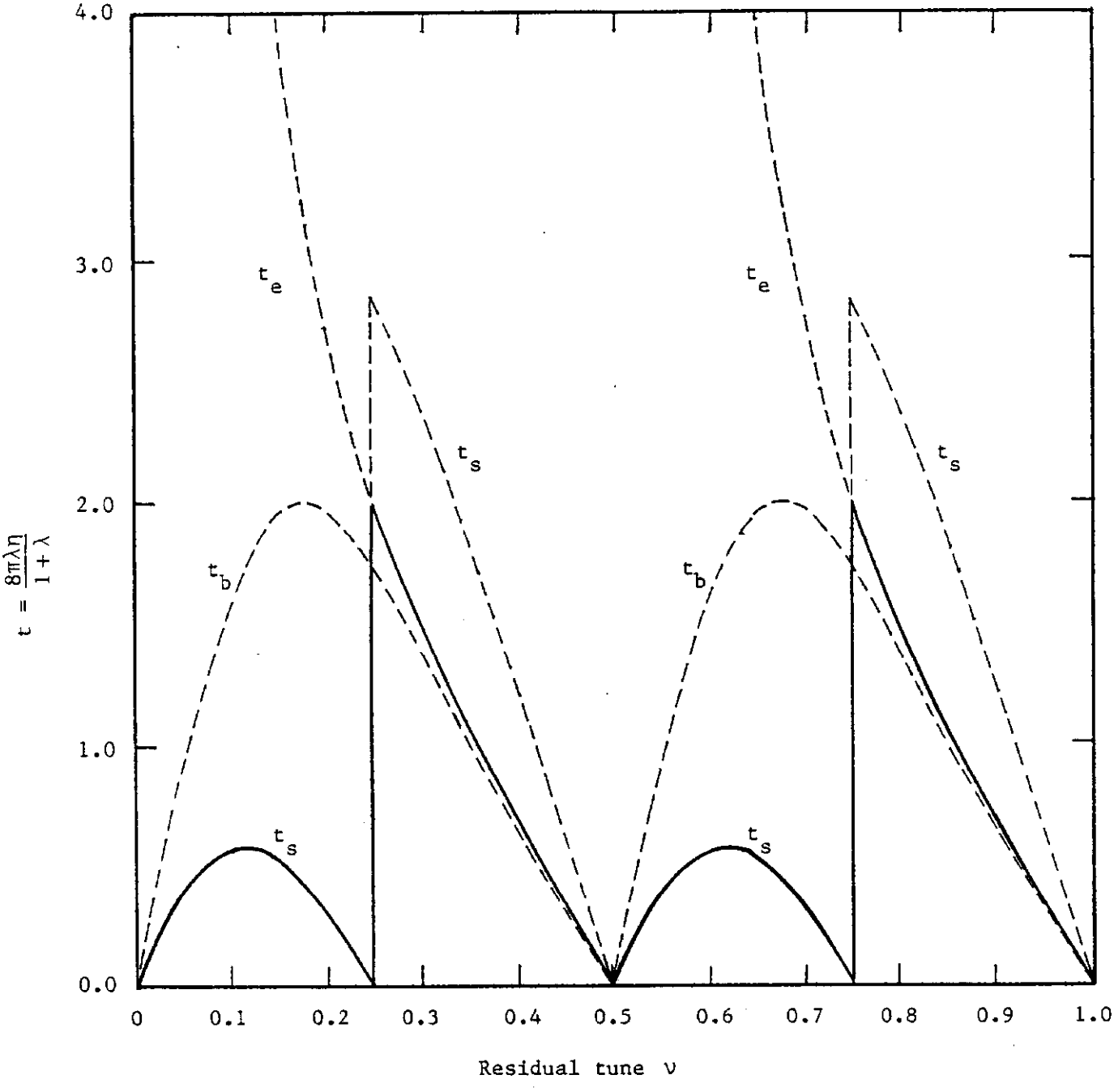

Figure 4. Stability diagram for linear beam-beam interactions. Only the region under the solid curve is stable. Bifurcation solution (stable or unstable) occurs when t is between t_b and t_e.

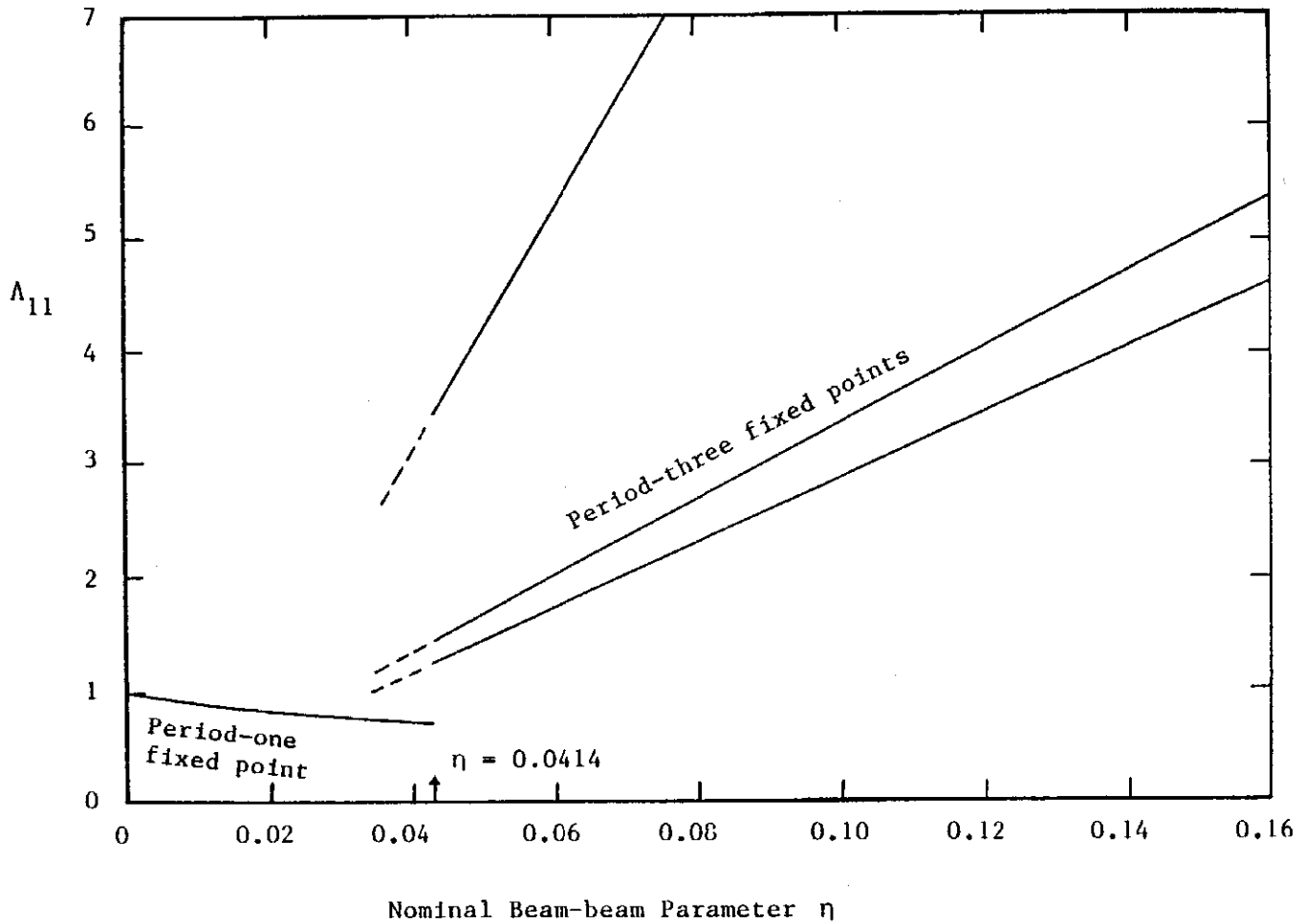

Figure 5. "Normalized" bunch emittance for residual tune $\nu = 0.15$ and damping time $T_0 = 142.9$ as a function of nominal beam-beam parameter η. The stable solution changes abruptly from period-one to period-three fixed points.

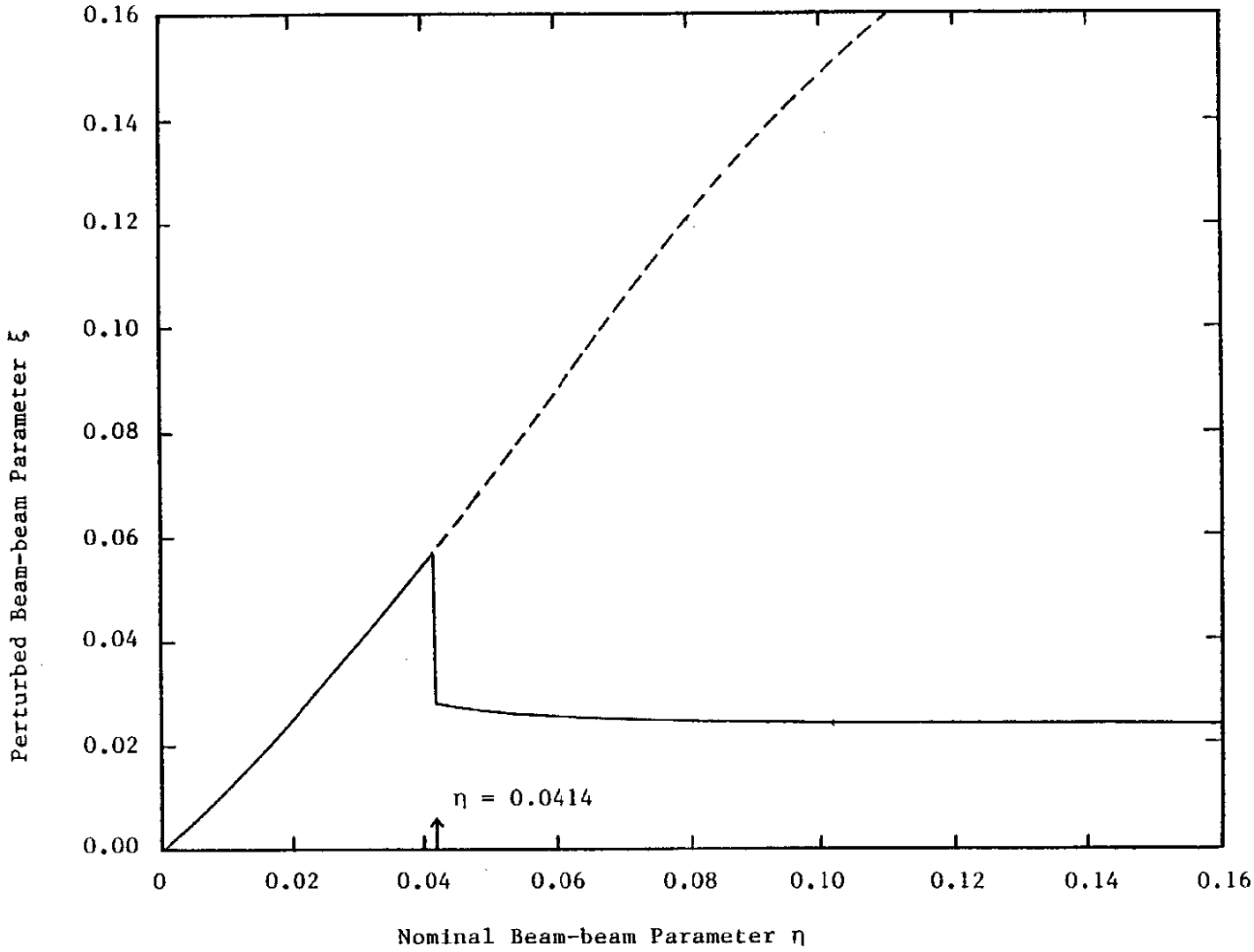

Figure 6. Perturbed beam-beam parameter ξ as a function of nominal beam-beam parameter η when the residual tune $\nu = 0.15$ and damping time $T_0 = 142.9$. The perturbed beam-beam parameter increases as t increases but drops abruptly to ~ 0.025 when $\eta > 0.0414$.

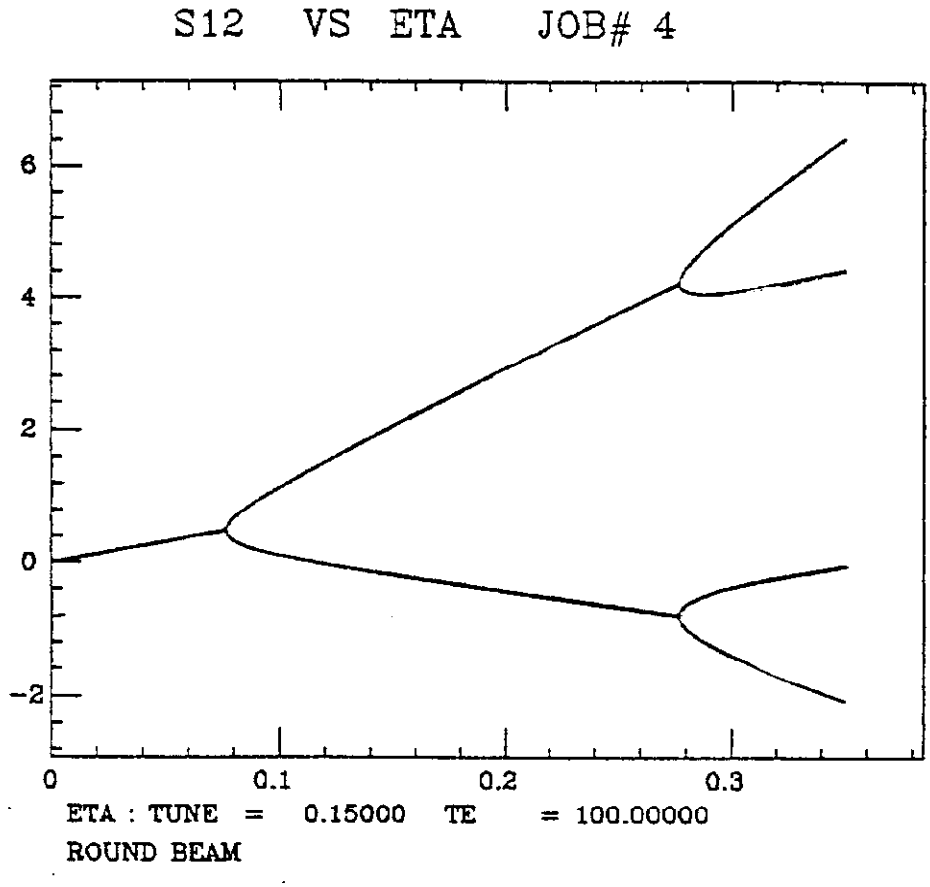

Figure 7. Tracking plot of Λ_{12} as a function of the nominal beam-beam parameter η with residual tune $\nu = 0.15$ and damping time $T_0 = 100$. In the tracking, we have tried to maintain $\Delta\Lambda_{ij} = \Delta\Lambda_{ij}$ all the time.

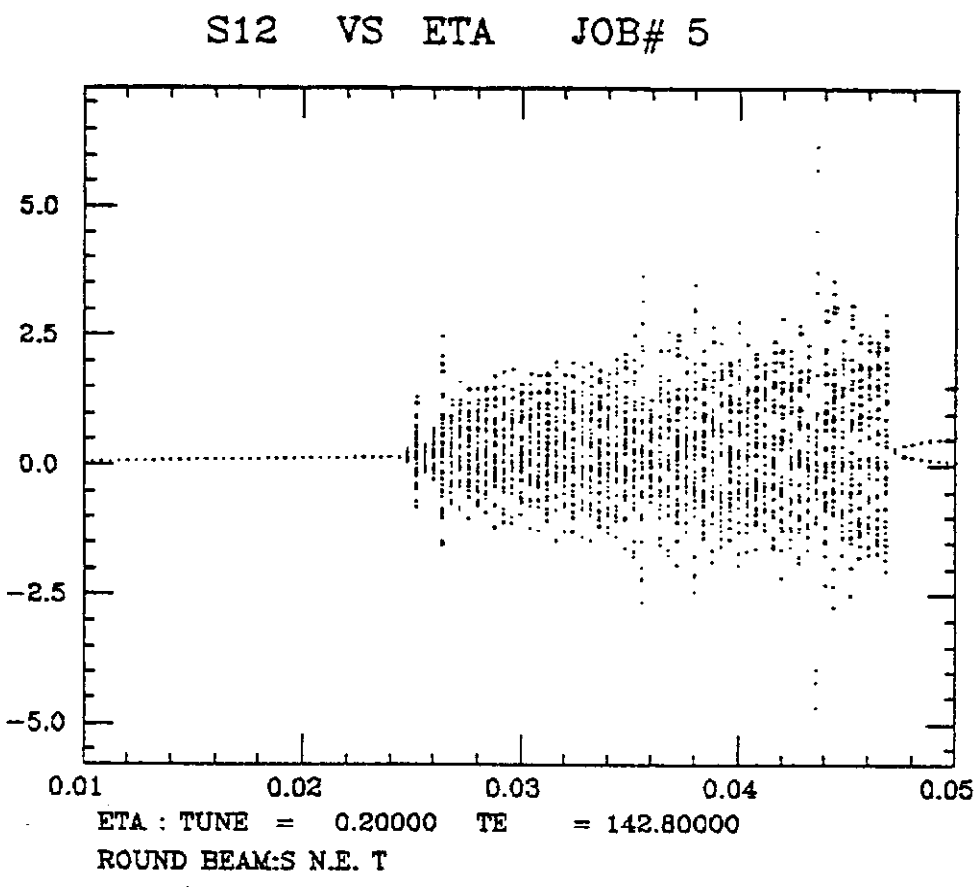

Figure 8. Tracking plot of Λ_{12} as a function of the nominal beam-beam parameter η with residual tune $\nu = 0.20$ and damping time $T_0 = 142.8$. Chaotic behavior can be seen when $t > t_s$.